



UNITED NATIONS
UNIVERSITY

UNU-GTP

Geothermal Training Programme

Orkustofnun, Grensasvegur 9,
IS-108 Reykjavik, Iceland

Reports 2015
Number 8

A STUDY ON DIFFERENT TWO-PHASE FLOW CORRELATIONS USED IN GEOTHERMAL WELLBORE MODELLING

Bryan T. Cacho

Energy Development Corporation - EDC
38/F One Corporate Centre Building
Julia Vargas corner Meralco Avenue
Ortigas Center, Pasig City, 1605
PHILIPPINES
cacho.bt@energy.com.ph

ABSTRACT

There are various flow correlations available to estimate the pressure drop associated with two-phase flow in a geothermal well. A number of previous studies on the different flow correlations have been conducted to assess their applicability in geothermal wellbore modelling. In this study, the performance of five flow correlations was evaluated and compared using discharge data from 39 geothermal wells that cover a wide range of wellhead conditions. The wellhead parameters were utilized to simulate the flowing pressure and temperature profiles using the wellbore simulator Simgwel. Different analyses were performed to identify which of these correlations would perform best depending on the condition of the fluid in the wellbore up to the wellhead.

1. INTRODUCTION

Geothermal wellbore modelling is one of the methods that reservoir engineers use for resource management decisions because it can provide vital information about the geothermal reservoir. It is the process of characterizing the behaviour of a geothermal well by reproducing the measured pressure and temperature profile and determining the relative contribution, fluid properties and fluid composition of each feed zone for a given discharge condition (Aunzo et al., 1991). Wellbore simulation can be used for optimizing the utilization of geothermal wells and improving reservoir models (Freeston and Gunn, 1993). Wellbore models are also being utilized to estimate improvements in well performance after carrying-out well interventions such as mechanical workover, relining of casing and acid injection (Fajardo and Malate, 2005). Based on its aforementioned applications, wellbore simulation is an important tool for resource optimization and management.

It is necessary to have a good understanding of the main aspects concerning the two-phase fluid flow in geothermal wells when performing wellbore simulations. Having in-depth knowledge about fluid flow can help predicting the pressure drop in the well more accurately and give better predictions if changes were to occur on mass flow or pressure in the well (Thórisdóttir, 2013). Various flow correlations have been developed to estimate the pressure drop in two-phase flow. These flow correlations greatly affect the simulated pressure drop in a geothermal well (Hsu and Graham, 1976). Accurately predicting the pressure drop in a geothermal well requires detailed information on:

- 1) Estimated feed zone contribution at a given wellhead condition;
- 2) Flash point location (used to determine the setting depth for calcite inhibition system in lieu of an actual survey);
- 3) Fluid velocity profile (required to predict required bottom hole assembly weight, throttling or threshold wellhead pressure to minimize erosion and sometimes to determine required throttling to run-in downhole tools); and
- 4) Fluid enthalpy changes.

All four aspects affect the simulated discharge parameters. Therefore, it is worthwhile to investigate the performance and applicability of these flow correlations. In this study, five two-phase flow correlations were used to predict the discharge pressure and temperature profiles of 39 geothermal wells using a wellbore simulator. The simulated pressure and temperature profiles were compared to the actual discharge data to evaluate and compare the performance of each flow correlation. The flow correlations used in this study are Orkiszewski, Armand, Duns and Ros, Hagedorn and Brown and Duns and Ros modified by Ros. The main objective of this study is to evaluate and compare the performance of these two-phase flow correlations and determine their applicability with given wellhead conditions.

2. THEORY ON TWO-PHASE FLOW IN GEOTHERMAL WELLS

In a high-temperature liquid-dominated reservoir, geothermal fluid generally undergoes flashing as it travels up through the wellbore. This flashing, which occurs due to pressure loss experienced by the fluid while travelling up through the wellbore, leads to two-phase flow. The pressure drop associated with two-phase fluid transport in a well is the sum of the pressure losses due to the frictional, gravitational and acceleration forces. In single-phase flow, the pressure drop can be easily determined because the fluid properties are well defined (Probst et al., 1992). However, in two-phase flow, accurately predicting the pressure drop is difficult because two-phase flows are complex and, under some conditions, the vapour moves with a higher velocity than the liquid. In addition, the velocity of the liquid phase along the casing wall of the wellbore can vary considerably over a short distance and resulting in variable friction loss. And under other conditions, the liquid is almost completely entrained in the gas and has very little friction loss due to contact with the casing wall. Therefore, the difference in velocity and the geometry of the two phases are very significant in predicting pressure drop in two-phase flow (Aunzo et al., 1991).

2.1 Single-phase flow

As mentioned above, pressure drop in single-phase flow through pipes can be easily estimated. In fluid mechanics literature by White (1979) the flow of single-phase fluid in pipes was investigated intensively. The flow calculations are performed with linear equations assuming that the fluid properties remain relatively constant (Björnsson, 1987). The components of the total pressure drop (pressure loss due to friction, gravity and acceleration) are given by:

$$\left[\frac{dP}{dz}\right]_{fri} = \frac{fG^2}{4r_w\rho} \quad (1)$$

$$\left[\frac{dP}{dz}\right]_{pot} = \rho g \sin\theta \quad (2)$$

$$\left[\frac{dP}{dz}\right]_{acc} = \frac{d(Gu)}{dL} \quad (3)$$

where $\left[\frac{dP}{dz}\right]_{fri}$ = Pressure drop component due to friction [Pa/m];
 $\left[\frac{dP}{dz}\right]_{pot}$ = Pressure drop component due to gravity [Pa/m];

- $\left[\frac{dP}{dz}\right]_{acc}$ = Pressure drop component due to acceleration [Pa/m];
 f = Friction factor;
 G = Mass flux [$\text{kg s}^{-1} \text{m}^{-2}$];
 r_w = Well radius [m];
 ρ = Density of fluid [kg/m^3];
 g = Gravitational constant [m/s^2];
 θ = Deviation angle from horizontal [degree]; and
 u = Average fluid velocity [m/s].

Thus, the total pressure drop equation can be written as:

$$\frac{dp}{dz} = \left[\frac{dP}{dz}\right]_{fri} + \left[\frac{dP}{dz}\right]_{pot} + \left[\frac{dP}{dz}\right]_{acc} \quad (4)$$

The friction factor f is given by White (1979):

If $Re < 2400$:

$$f = \frac{64}{Re} \quad (5)$$

If $Re \geq 2400$:

$$\frac{1}{f} = -2.0 \log_{10} \left[\frac{\epsilon}{3.7(2r_w)} + \frac{2.51}{Re f^{0.5}} \right] \quad (6)$$

where Re = Reynold's number; and

ϵ = Pipe roughness [m].

2.1.1 The continuity equation

The continuity equation describes the transport of conserved quantity (conservation of mass):

$$\frac{d}{dz}(\dot{m}) = 0 \quad (7)$$

If the diameter of the pipe is assumed to be constant, Equation 7 could be written in terms of cross sectional area of the pipe and fluid density as:

$$\frac{d}{dz}(\rho u) = 0 \quad (8)$$

2.1.2 The energy equation

From the first law of thermodynamics, the energy conservation equation contains a kinetic, potential and enthalpy part. The first term represents the change in kinetic energy due to the change in velocity, the second term is the change in potential energy as a result of change in elevation and the third term is the change in enthalpy:

$$\dot{m}u \frac{du}{dz} + \dot{m}g + \dot{m} \frac{dh}{dz} + \dot{Q} = 0 \quad (9)$$

where \dot{Q} = Heat loss from the pipe per unit length [W/m]; and

h = Enthalpy of the fluid [kJ/kg].

2.1.3 The momentum equation

The momentum equation is divided into four terms: inertia, pressure changes, hydrostatic pressure and

head losses. The first term represents the change in inertia caused by velocity change, the second term is the pressure change of the fluid, the third term is the change in hydrostatic pressure and the last term is the head loss due to friction. The term $|u|u$ is used in order to consider the flow in both directions since the head loss is always in the direction of the flow:

$$\rho u \frac{du}{dz} + \frac{dp}{dz} + \rho g + \frac{\rho f}{2d} |u|u = 0 \quad (10)$$

where d = Diameter of the pipe [m].

2.1.4 Matrix form of the equations

The equations in the last three subsections need to be solved simultaneously. In order to do so, the equations were assembled in matrix form by Pálsson (2011). The matrix can also be solved using numerical integration from the bottom of the well to the top.

$$\begin{bmatrix} \rho & u \frac{\partial \rho}{\partial p} & u \frac{\partial \rho}{\partial h} \\ \dot{m}u & 0 & \dot{m} \\ \rho u & 1 & 0 \end{bmatrix} \frac{d}{dz} \begin{bmatrix} u \\ p \\ h \end{bmatrix} + \begin{bmatrix} 0 \\ \dot{m}g + \dot{Q} \\ \rho g + \frac{\rho f}{2d} |u|u \end{bmatrix} = \begin{bmatrix} 0 \\ 0 \\ 0 \end{bmatrix} \quad (11)$$

2.2 Two-phase flow

All the basic laws of fluid mechanics also apply to two-phase flow. However, equations describing two-phase flow are more complicated than those describing single-phase flow because the liquid and vapour phases have different thermodynamic properties (Thórisdóttir, 2013). The three main equations which are continuity, momentum, and energy will have to take both phases into account. To characterize two-phase flow, two important auxiliary parameters, steam mass fraction and void fraction, are introduced (Pálsson, 2011). The steam mass fraction is defined as the ratio of the mass of steam to the total mass of the mixture. The steam mass fraction x , also called as dryness, is given as:

$$x = \frac{\dot{m}_g}{\dot{m}} = \frac{\dot{m}_g}{\dot{m}_g + \dot{m}_l} \quad (12)$$

where \dot{m}_g = Mass of steam or vapour [kg/s];
 \dot{m}_l = Mass of liquid [kg/s]; and
 \dot{m} = Total mass of the mixture [kg/s].

The steam mass fraction can also be expressed in terms of enthalpy:

$$x = \frac{h - h_l}{h_g - h_l} \quad (13)$$

where h_g = Enthalpy of the steam or vapour [kJ/kg]; and
 h_l = Enthalpy of the liquid [kJ/kg].

Void fraction α is defined as the fraction between the area of steam and the total area of a given cross-section of a pipe (Pálsson, 2011). It is also called steam saturation and expressed as:

$$\alpha = \frac{A_g}{A} = \frac{A_g}{A_g + A_l} \quad (14)$$

where A = Cross-sectional area of the well [m²];
 A_g = Cross-sectional area occupied by vapour [m²]; and
 A_l = Cross-sectional area occupied by liquid [m²].

In two-phase separated flow, there are two velocities present, liquid velocity u_l and vapour velocity u_v . Pálsson (2011) simplified the expression of flow velocities into a single variable, u . Where u is defined as the velocity that would be experienced if the liquid was flowing alone in the pipe, but with the same mass flow as the total flow:

$$u = \frac{\dot{m}}{\rho_l A} \quad (15)$$

Pálsson (2011) also incorporated u and x to the actual velocities where liquid velocity becomes:

$$u_l = \frac{\dot{m}_l}{\rho_l A_l} = \frac{(1-x)\dot{m}}{\rho_l(1-\alpha)A} = \frac{1-x}{1-\alpha}u \quad (16)$$

and the vapour velocity:

$$u_v = \frac{\dot{m}_g}{\rho_g A_g} = \frac{x\dot{m}}{\rho_g \alpha A} = \frac{x\rho_l}{\alpha\rho_g}u \quad (17)$$

where ρ_l = Density of the liquid [kg/m^3]; and
 ρ_g = Density of the vapour [kg/m^3].

2.2.1 The continuity equation

The continuity equation for two-phase flow consists of liquid and vapour phases. Assuming that the pipe diameter is constant, the equation can be written as:

$$\frac{d}{dz}(\dot{m}_l + \dot{m}_v) = \frac{d}{dz}(\rho_l u_l A_l + \rho_g u_g A_g) = 0 \quad (18)$$

Equation 18 was also simplified by Pálsson (2011) using the void fraction definition:

$$\frac{d}{dz}(\rho_l u_l (1-\alpha) + \rho_g u_g \alpha) = 0 \quad (19)$$

$$\frac{d}{dz}(\rho_l (1-x)u + \rho_l x u) = 0 \quad (19)$$

$$\frac{d}{dz}(\rho_l u) = 0 \quad (20)$$

2.2.2 The energy equation

The energy equation for two-phase flow can be written as:

$$\frac{d}{dz} \left(\dot{m}_l \left(\frac{u_l^2}{2} + gz + h_l \right) + \dot{m}_v \left(\frac{u_g^2}{2} + gz + h_g \right) \right) + \dot{Q} = 0 \quad (21)$$

Introducing γ in the equation and following the derivation of Pálsson (2011) would give:

$$\gamma = \frac{(1-x)^3}{(1-\alpha)^2} + \frac{\rho_l^2 x^3}{\rho_g^2 \alpha^2} \quad (22)$$

$$\gamma u \frac{du}{dz} + \frac{u^2 \partial \gamma \partial p}{2 \partial p \partial z} + \left(1 + \frac{u^2 \partial \gamma}{2 \partial h} \right) \frac{dh}{dz} + g + \frac{\dot{Q}}{\dot{m}} = 0 \quad (23)$$

2.2.3 The momentum equation

The momentum equation in two-phase flow has to consider the inertial part and the gravitational part where the density has to be an averaged value with respect to the void fraction (Pálsson, 2011):

$$\rho_\alpha = (1 - \alpha)\rho_l + \alpha\rho_g \quad (24)$$

Hence, the momentum equation can be written as:

$$\frac{d}{dz}(\dot{m}_l u_l + \dot{m}_g u_g) + A \frac{dp}{dz} + ((1 - \alpha)\rho_l + \alpha\rho_g)gA + \Phi^2 \frac{\rho_l f A}{2d} u^2 \quad (25)$$

where Φ^2 = Correction factor for the frictional pressure loss in two-phase flow.

The momentum equation is simplified by introducing η :

$$\eta = \frac{(1 - x)^2}{1 - \alpha} + \frac{\rho_l x^2}{\rho_g \alpha} \quad (26)$$

Finally, the momentum equation can be written as:

$$\begin{aligned} \eta\rho_l u \frac{du}{dz} + \left(1 + \rho_l u^2 \frac{\partial \eta}{\partial p} + \eta u^2 \frac{\partial \rho_l}{\partial p}\right) \frac{dp}{dz} + \rho_l u^2 \frac{\partial \eta}{\partial h} \frac{dh}{dz} + ((1 - \alpha)\rho_l + \alpha\rho_g)g \\ + \frac{\Phi^2 \rho_l f}{2d} u^2 = 0 \end{aligned} \quad (27)$$

2.2.4 Matrix form of the equations

The three governing equations were assembled in a similar manner as in single-phase flow by Pálsson (2011) in matrix form which can also be solved by using numerical integration from the bottom to the top of the well.

$$\begin{aligned} \begin{bmatrix} \rho_l & u \frac{\partial \rho_l}{\partial p} & 0 \\ \gamma u & \frac{u^2}{2} \frac{\partial \gamma}{\partial p} & \left(1 + \frac{u^2}{2} \frac{\partial \gamma}{\partial h}\right) \frac{d}{dz} \begin{bmatrix} u \\ p \\ h \end{bmatrix} \\ \eta\rho_l u & \left(1 + \rho_l u^2 \frac{\partial \eta}{\partial p} + \eta u^2 \frac{\partial \rho_l}{\partial p}\right) & \rho_l u^2 \frac{\partial \eta}{\partial h} \end{bmatrix} \\ + \begin{bmatrix} 0 \\ g + \frac{\dot{Q}}{\dot{m}} \\ ((1 - \alpha)\rho_l + \alpha\rho_g)g + \frac{\Phi^2 \rho_l f}{2d} u^2 \end{bmatrix} = \begin{bmatrix} 0 \\ 0 \\ 0 \end{bmatrix} \end{aligned} \quad (28)$$

2.2.5 Liquid holdup

Liquid holdup (H_l) is defined as the fraction of a unit volume of pipe which is occupied by liquid at same instant (Carrascal, 1996). It is expressed as:

$$H_l = \frac{\text{volume of liquid in a pipe segment}}{\text{volume of pipe segment}} \quad (29)$$

3. TWO-PHASE FLOW CORRELATIONS

Many empirical correlations and models have been developed to estimate the pressure drop associated with two-phase flow in geothermal wells (Probst et al., 1992). These correlations use different methods in calculating the three components of the total pressure gradient (see Equation 4). Some of these correlations will be described later.

Two-phase flow models were divided into two categories: homogenous and separate flow models. The assumption in homogenous flow model is that the liquid and vapour phases travel at the same velocity and the slippage between the phases are ignored. In separated flow models, it is considered that the vapour phase flows faster than the liquid phase and that the phases flow concurrently (Gudmundsdóttir, 2012). The difference between liquid and vapour velocities is called "slip velocity" (Probst et al., 1992). According to Björnsson (1987), it is customary to use the method of separated flow models where the flow of liquid and vapour are treated separately using the well-established theory of single-phase flow. Then, the equations for the two phases are extended for two-phase flows using empirical correlations. These empirical correlations are also called two-phase flow correlations.

3.1 Orkiszewski correlation

The Orkiszewski correlation (Orkiszewski, 1967) is based on the study of several published correlations used to determine the pressure drop in oil and gas systems. Orkiszewski selected different two-phase flow correlations and evaluated them by comparing correlation predictions to actual data. A total of 148 wells were used in the investigation. The results show that no single correlation was accurate enough to predict the pressure gradient in a well for a wide set of different flow conditions.

Two-phase flow correlations were classified by Orkiszewski (1967) according to their similarity in theoretical concepts and separated into three categories:

1. The liquid holdup is neglected in the determination of the mixture density which is just corrected by pressure and temperature. The liquid holdup and the pressure losses are correlated in an empirical friction factor. Flow regimes are neglected.
2. The liquid holdup is considered in the calculation of the mixture density. It is correlated separately or in combination with friction losses. The friction losses are calculated using the properties of the mixture. Flow regimes are neglected.
3. The liquid holdup is used to calculate the mixture density. The liquid holdup is determined using the concept of slip velocity (difference between gas and liquid velocities). The friction losses are determined using the continuous phase. Flow regimes are considered.

There are four flow regimes that were considered in the Orkiszewski correlation. These flow regimes are: bubble, slug, transition (slug-annular) and mist. Orkiszewski (1967) used different methods for predicting pressure drop and chose which among them is the most appropriate to use for each flow regime. For bubble flow, Griffith-Wallis (1961) correlation was used without any modifications done in the correlation. For slug flow, the same correlation was used but it was modified because it is not reliable in the higher flow rate range of slug. The modification of the Griffith-Wallis correlation (for the slug flow) included a parameter for the liquid distribution, the liquid film and the liquid entrained in the gas bubble. This parameter accounts for the liquid holdup at the higher flow velocities. Orkiszewski used the data from the Hagedorn and Brown (1965) model to evaluate the liquid distribution coefficient or holdup (Bellarby, 2009). For mist flow, the Duns and Ros correlation (1963) was used. Flow correlations that were used in Orkiszewski method for different flow regimes are listed in Table 1.

TABLE 1: Correlations used in Orkiszewski method

Method / correlation	Flow regime
Griffith	Bubble
Griffith and Wallis	Slug (density term)
Orkiszewski	Slug (friction gradient term)
Duns and Ros	Transition
Duns and Ros	Mist or annular

3.1.1 Flow regimes considered in Orkiszewski correlation

In the case of two-phase flow, the distribution of liquid and gas phases may vary depending on the velocity, the inclination of the well and the amount of each fluid. Flow regimes can be considered as the distribution of each phase with respect to each other in a well. Determining the flow regimes in a vertical well is much easier than in a horizontal well because in the horizontal flow pattern, the phases tend to separate due to gravity. For a two-phase fluid flowing up through an incline pipe, the flow pattern is slug or mist for most of the cases (Carrascal, 1996). As mentioned above, there are four flow regimes that were considered by Orkiszewski (1967), their names and descriptions are as follows:

- *Bubble* - In this flow regime, the liquid phase is the continuous phase and occupies most of the pipe volume. The gas is distributed in the pipe in form of bubbles that have different sizes and moving in different velocities. The effect of gas on the pressure gradient is small because of its density value. Therefore, the liquid phase is decisive in the pressure gradient calculation.
- *Slug* - The liquid phase in this regime remains as the continuous phase, but the bubbles have increased in number and form a single bubble that may have a size close to the pipe diameter. The bubbles are surrounded by a liquid film. The liquid around the film may move upward (in direction of bulk flow) or it may move downward. The gas bubbles have higher velocity than the liquid. Both liquid and gas contributes in the total pressure gradient.
- *Transition* - In this regime, the gas phase becomes the continuous phase and some liquid is entrained as small droplets into gaseous phase. The gas phase is more dominant than the liquid phase. Thus, the gas has a greater influence on the total pressure gradient than the liquid.
- *Mist* - The gas phase is the continuous phase and the liquid is entrained in the gas where gas is the predominant factor. The gaseous phase controls the pressure gradient and liquid causes secondary effects.

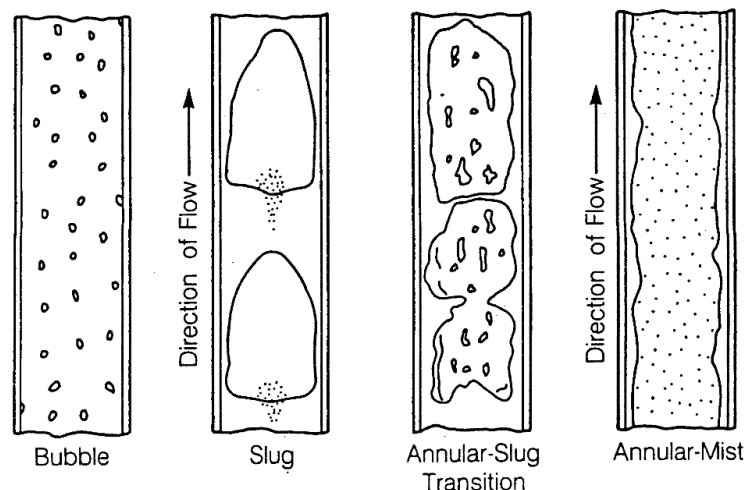


FIGURE 1: Illustration of the four flow regimes in the Orkiszewski correlation (Orkiszewski, 1967)

An illustration of how the fluid looks in different flow regimes (bubble, slug, transition and mist), taken from Orkiszewski (1967), is presented in Figure 1.

3.2 Duns and Ros correlation

The Duns and Ros (1963) correlation is the result of intensive laboratory experiments. About 4,000 two-phase flow tests were conducted in a 185 ft. high vertical-flow loop. Pipe diameters used are ranging from 1.3 to 5.6 inches. Most of the tests were near atmospheric conditions using air (for the gas phase) and liquid hydrocarbons or water (for the liquid phase). The authors expressed the energy equation as a pressure balance equation. They defined three terms in the pressure balance equation: the static gradient term, the wall friction gradient term and the acceleration gradient term. In the static gradient term, the effects of liquid holdup were considered and were kept separated from the effects of friction (Carrascal, 1996). Duns and Ros (1963) developed a flow regime map which is used as the basis of parameters of superficial gas and liquid velocities. The flow regime map is divided into three regions and the liquid holdup is calculated differently in each region (Bellarby, 2009). The three regions are determined by the

continuity, or lack of continuity, of the liquid and gas phases. These regions were defined by Duns and Ros (1963) as follows:

- *Region I* - The liquid phase is continuous and bubble flow, plug flow and part of the froth flow regime exists.
- *Region II* - In this region, the phases of liquid and gas alternate. The region covers slug flow and the remainder of the froth flow regime.
- *Region III* - The gas is in a continuous phase and the mist flow regime exists.

The diagrams and regions are illustrated in Figure 2. There is also a transition zone between regions II and III (see Figure 2). The Duns and Ros correlation is widely used for pressure drop prediction in mist flow regime (Bellarby, 2009). The correlation was developed for oil and gas mixtures, however, the authors claim that the method should also be accurate for water and gas mixtures (Probst et al., 1992).

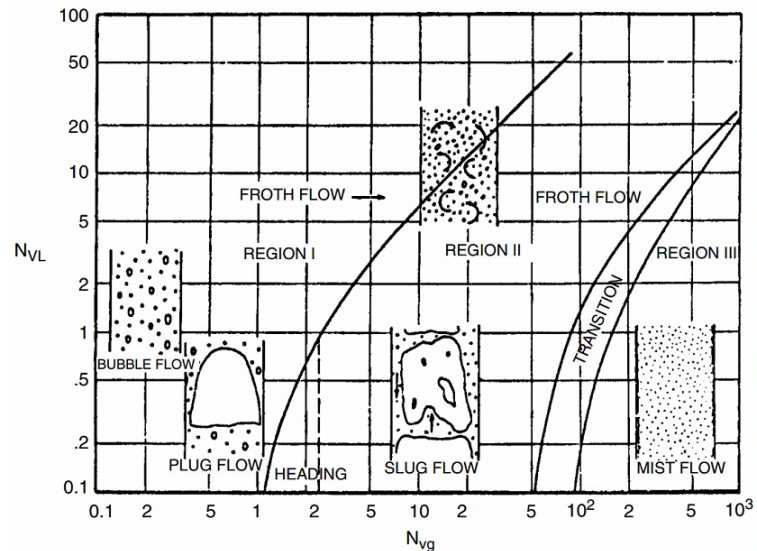


FIGURE 2: Region of occurrence of different flow regimes as described by Duns and Ros (1963); figure adapted from Lyons (2010)

3.3 Duns and Ros modified by Ros correlation

Duns and Ros modified by Ros correlation was developed from tests on a vertical pipe using air-water and air-liquid hydrocarbon mixtures. The only difference between this correlation and the Duns and Ros correlation is the treatment of pressure drop due to acceleration and friction. Duns and Ros modified by Ros correlation uses a two-phase multiplier based on Martinelli and Nelson and modified by Chisholm, while Duns and Ros correlation uses their own two-phase multiplier to correct the single-phase pressure drop due to friction (McGuinness, 2014).

3.4 Hagedorn and Brown correlation

Hagedorn and Brown (1965) developed an empirical correlation using a small-diameter, 1500-ft. vertical experimental well. In the experimental analysis, tubing diameters ranging from 1 to 2 in. were considered along with five different fluid types, namely water and four types of oil with viscosities ranging between 10 and 110 cP (at 80°F). This correlation does not consider different flow regimes. The liquid holdup is used as a correlating parameter in the calculation of the total pressure drop for an incremental length of pipe. Nevertheless, this correlation is effectively a prediction for slug flow, although further study was done to verify whether the flow was in the bubble flow regime (Lyons, 2010).

Having been one of the frequently used correlations, Hagedorn and Brown method has been derived several times subsequently, ensuring that the predicted holdup would not go below the no-slip hold-up in the calculations as this tends to produce better results (Bellarby, 2009).

Furthermore, this correlation was generated using data measured for a wide range of gas-liquid ratios and differing fluid properties. Hence, this correlation is commonly used in oil wells including those with

pumps. In spite of their increasing gas to liquid ratios, gas-lifted wells still frequently produce slug flow and the Hagedorn and Brown correlation therefore, remains applicable (Ravindran and Horne, 1993).

3.5 Armand correlation

The Armand (1946) correlation is one of the first correlations for predicting the void fraction while considering the non-homogenous nature of two-phase flow (Aunzo et al., 1991). Also, Armand's empirical correlation was used to calculate the velocities of gas and liquid phases that are needed in the evaluation of momentum flux and energy equations (Bhat et al., 2005). According to the study of Spedding and Chen (1982), Armand correlation only applies to the bubble and slug flow regimes.

3.6 Previous studies

Many researchers have conducted studies on the different correlations used in various two-phase flow, or pressure drop models. Gould (1974) is one of the first researchers who assessed the applicability of different pressure drop models to the geothermal industry. Gould evaluated the performance of three correlations namely, Hagedorn and Brown (1965), Aziz (1972) and Orkiszewski (1967) correlations, simulating data primarily taken from the wells of Wairakei and Broadlands fields in New Zealand. However, Gould only considered the effect of dissolved solids and ignored the effects of non-condensable gasses. Consequently, Gould provisionally concluded that one modification of Hagedorn and Brown correlation was the most consistent in performance.

Another pair of investigators is Ambastha and Gudmundsson (1986) who noted that the general applicability of flow correlations cannot be demonstrated if a number of pressure drop models are compared on a single or only few data sets. The authors decided to check on which geothermal conditions Orkiszewski (1967) correlation performs satisfactorily by collecting well test data from 10 geothermal wells demonstrating a wide range of characteristics (although pure water was assumed in all cases). Eventually, the authors were able to conclude that the Orkiszewski (1967) correlation is generally applicable; however, it obtains better results when the steam mass flux (steam flow per unit area) is greater than $100 \text{ kg s}^{-1} \text{ m}^{-2}$.

A comparison of Orkiszewski (1967) correlation with another correlation was the study of Tanaka and Nishi (1988). There the authors matched the Orkiszewski (1967) correlation with another correlation for sixteen tests of eight wells, thirteen of which were incorporated with carbon dioxide content. All production data have wellhead dryness fractions of 10% or less. With this, Tanaka and Nishi observed that the Orkiszewski correlation did not perform satisfactorily. On the other hand, Freeston and Hadgu (1988) compared five wellbore simulators, three of which were based on the Orkiszewski (1967) correlation and one being the simulator developed by Barelli et al. (1982) which was the only one capable of handling non-condensable gases. Freeston and Hadgu (1988) tested the simulators on production data from eleven wells with broad and different characteristics and concluded that none of the five simulators were applicable to all conditions.

4. PERFORMANCE EVALUATION OF FLOW CORRELATIONS

4.1 Geothermal well data

Prior to the evaluation of flow correlations, discharge data from 39 two-phase production wells were collected. The geothermal wells are located in five geothermal fields in the Philippines: BacMan, Leyte, Mindanao, Northern Negros and Southern Negros. Additionally, one well located in Reykjanes, Iceland, was used. The data that were utilized in this study cover a wide range of wellhead conditions. The

wellhead pressure ranges from 5 to 60 bar-a, the enthalpy from 900 to 2500 kJ/kg and the total mass flowrate from 7 to 70 kg/s. Most of the wells are standard diameter wellbores (9 5/8" production casing diameter). The discharge data, wellhead diameter and depth of the wells are shown in Table 2.

TABLE 2: Discharge test data used for the flow correlation comparisons

Well	Mass flow (kg/s)	Wellhead dryness (%)	Depth (m)	Wellhead diameter (in)	Well	Mass flow (kg/s)	Wellhead dryness (%)	Depth (m)	Wellhead diameter (in)
1	Moderate	Low	1927	13 3/8"	20	Low	Medium	1210	13 3/8"
1.1	Moderate	Low	1927	13 3/8"	21	High	Low	1731	9 5/8"
2	Moderate	Medium	1179	9 5/8"	22	Moderate	Medium	623	9 5/8"
3	Moderate	Low	1334	13 3/8"	23	Low	Low	609	9 5/8"
4*	Low	Low	1460	9 5/8"	24	Low	Medium	599	9 5/8"
5	Low	Medium	652	9 5/8"	25	Low	Medium	654	9 5/8"
6	High	Low	862	13 3/8"	26	Low	Low	637	9 5/8"
7	High	Low	1561	9 5/8"	27	Low	Medium	1454	9 5/8"
8	Low	Low	667	9 5/8"	28	Low	Low	1283	9 5/8"
9	Low	Medium	902	9 5/8"	29	Low	Low	1285	9 5/8"
10	Moderate	Low	1947	13 3/8"	30	Moderate	Low	963	9 5/8"
11	Low	Low	1955	9 5/8"	31	High	Low	1176	9 5/8"
12	Low	Medium	1220	13 3/8"	32	Moderate	Low	1760	9 5/8"
13	High	Low	601	9 5/8"	33	Moderate	Low	1407	9 5/8"
14	Moderate	Low	1014	9 5/8"	34	High	Low	1056	9 5/8"
15	Low	Medium	733	9 5/8"	35	Low	Medium	1610	9 5/8"
16*	Low	Low	680	9 5/8"	36	Moderate	Low	1224	9 5/8"
17	Moderate	Low	862	9 5/8"	37	Moderate	Low	1260	9 5/8"
18	Moderate	Low	1001	9 5/8"	38	Moderate	Low	1747	9 5/8"
19	High	Low	1747	9 5/8"	39	Moderate	Low	1430	9 5/8"

* perforated wells

The total mass flowrates were classified as low (< 20 kg/s), moderate (20 - 40 kg/s) and high (> 40 kg/s). Wellhead dryness was classified as low (< 1500 kJ/kg), medium (1500 - 2500 kJ/kg) and high (> 2500 kJ/kg). The depth indicated in Table 2 is not the total depth of the well. The depth considered in this study is the depth where the top of the slotted liner (TOL) is located. And for perforated wells, the depth was set just above the perforated section. Also, note that one of the wells has two sets of discharge data. Both data were used, named Well 1 and Well 1.1.

The parameters used for evaluating the performance of the flow correlations are summarized below:

- Wellhead parameters (wellhead pressure, total mass flow and enthalpy);
- Casing geometry of the well;
- Pressure and temperature logs during discharge.

The total mass flowrate and enthalpy of the wells at the wellhead were calculated using the James lip pressure method while pressure and temperature logs were taken using Kuster pressure and temperature gauge. For some of the wells, flowing pressure and temperature were measured using a memory type PTS (Pressure-Temperature-Spinner) measuring tool.

4.2 Wellbore simulation

The flowing pressure and temperature profiles in the cased portion of the wells were simulated using the earliest version of wellbore simulator Simgwel (ver. 9.21) developed by Marsan Consulting, Ltd. and Energy Development Corporation (Marquez et al., 2015). The core of Simgwel is based on the research tool GWELL and completely written in Fortran95. The wellbore simulator solves coupled steady-state mass, momentum and energy conservation equations for liquid, vapour and two-phase fluids containing carbon dioxide up a geothermal well (McGuinness, 2013). The capabilities of Simgwel as enumerated by Marquez et al. (2015) are:

- 1) Models liquid, steam and two-phase fluid flow where CO₂ content is considered;
- 2) Considering of the effect of heat transfer between the reservoir and the well;
- 3) Giving options for using different parameters in well geometry (i.e. roughness, inner diameter of casing or liner and deviation of the well);
- 4) Performing feed zone to wellhead and wellhead to feed zone simulations for single- or multi-feed production and injection wellbore models;
- 5) Producing simulated liquid and vapour velocities, flash point, flow pattern or flow regime, mass fraction of CO₂, enthalpy, static and dynamic steam fraction, flowing pressure and temperature across a well's depth;
- 6) Providing well's output for different wellhead pressures using estimated deliverability parameters (i.e. steam coefficient, linear drawdown factor, quadratic drawdown coefficient and viscosity-independent productivity index) given other feed parameters (i.e. reservoir pressure, mass flow and enthalpy);
- 7) Giving data points and graphical plots of simulated flowing pressures and temperatures, fluid velocities and bore output curves; and
- 8) Considering setting of the bottom hole pressure range of the simulated output curve.

The wellhead parameters in Table 2 were utilized to simulate the flowing pressure and temperature profiles using the five two-phase flow correlations: Orkiszewski (1967), Armand (1946), Duns and Ros (1963), Hagedorn and Brown (1965) and Duns and Ros modification by Ros (1961). Top-down simulations were performed wherein the calculations start from the wellhead down to TOL (or just above the shallowest feed, for perforated wells). Simulations only covered the cased-off section of the wells to limit the number of simulation variables that need to be controlled and to remove modeller bias that may result from modeller inputs of feed contribution and enthalpy. Modeller bias in the feed zone inputs is a concern because most of the studied wells do not have spinner data making it difficult to estimate the mass flow distribution across the feed zones. The effects of heat loss or gain from the formation to wellbore were also ignored. It is also assumed that the casing of the wells is clear from obstruction and scaling. The casing roughness assumed for all of the wells is 46 μm . Probst et al. (1992) stated that wellbore roughness is significant to the calculation of pressure drop because as the enthalpy of the fluid increases, the frictional component of the pressure drop also increases. A minimal mass fraction of CO₂ content (~ 0.001) was assumed in all simulations. This is a reasonable value, since it is a little less than the equilibrium value for water in contact with air at atmospheric condition (McGuinness, 2014).

4.3 Comparison of simulated and measured flowing profiles

To measure the accuracy of the flow correlations, the error between the measured and simulated flowing pressure and temperature profiles are calculated at every 15 m depth interval. The error is defined as:

$$e_i = \text{measured value} - \text{predicted value} \quad (30)$$

The calculated errors are used to apply the method of root-mean-square error (RMSE). The root-mean-square error is mostly used to measure the differences between values predicted by a model and the values actually measured or observed (Koehler and Koehler, 2006):

$$RMSE = \sqrt{\frac{1}{n} \sum_{i=1}^n e_i^2} \quad (31)$$

Then, the average of the pressure and temperature RMS-error is assumed to be the total error and used as the basis for evaluating the performance of each flow correlation:

$$\text{Total error} = \frac{RMSE_{\text{press.}} + RMSE_{\text{temp.}}}{2} \quad (32)$$

The correlation with the lowest total error would be the best match for that specific well. It is also possible that two or more correlations could give the best match on the pressure and temperature profile of the well. An example of that case is illustrated in Figure 3.

Figure 3 shows the plots of the measured and simulated temperature and pressure values of well 39 using five correlations. In this case, the Orkiszewski, and the Duns and Ros (modified by Ros) correlations performed equally well.

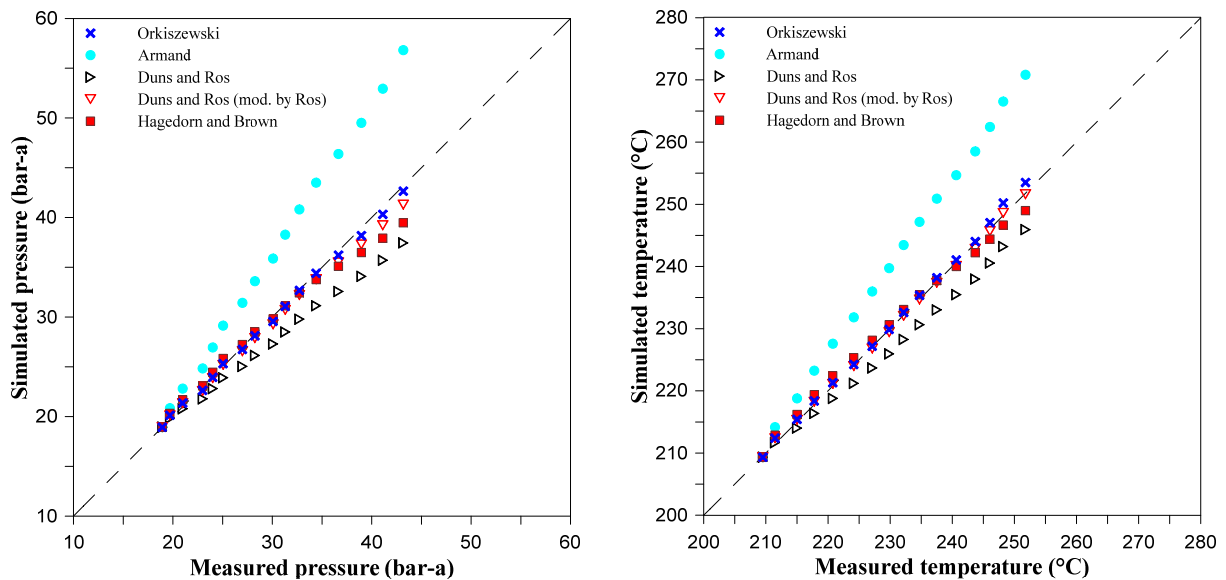


FIGURE 3: Measured vs. simulated pressure and temperature from wellhead to the top of slotted liner of well 39

4.4 Performance of flow correlations based on the number of wells matched

The performance of flow correlations was first evaluated based on the number of wells matched. The number of wells matched by each correlation and the mean error (based on wells matched) are summarized in Table 3. The results show that the Orkiszewski correlation matched 10 wells in which wellhead pressure is ranging from 10 to 50 bar-a and a total mass flow rate ranging from 7 to 70 kg/s (same as the data sets range of mass flow rate). It is also noted that the Orkiszewski correlation has the lowest mean error based on the results. The Armand correlation, on the other hand, matched 7 wells having a wellhead pressure ranging from 10 to 40 bar-a and mass flow rate ranging from 10 to 40 kg/s. However, the Armand correlation's performance is very poor based on both its number of wells matched and mean error.

TABLE 3: Number of wells best matched by the flow correlations based on average pressure and temperature RMS-error

Flow correlation	Number of best-matches	Mean error of best-matches (bar-a °C)
Orkiszewski	10	4.3
Armand	7	8.1
Duns and Ros	14	6.4
Duns and Ros (mod. by Ros)	12	4.7
Hagedorn and Brown	13	8.4

The Duns and Ros correlation performed the best among the tested correlations based on the total number of wells matched. Wells matched using this correlation have a wellhead pressure ranging from

5 to 30 bar-a and a mass flow rate ranging from 10 to 70 kg/s. As for the Duns and Ros (modified by Ros) correlation, it performed well in simulating flowing pressure and temperature profiles of wells having wellhead pressure within the range of 10 - 40 bar-a and mass flow rate within the range of 10 - 70 kg/s. Lastly, the Hagedorn and Brown correlation also performed well based on the number of wells matched, though its mean error is considerably higher. The wells matched by this correlation have wellhead pressure ranging from 8 to 60 bar-a and a mass flow rate ranging from 10 to 60 kg/s.

4.5 Performance of flow correlations based on error distribution

The histogram of the average RMS-errors of each flow correlations were constructed to further evaluate and compare their performances based on the distribution of the errors produced by each correlation. In the paper of Probst et al. (1992), it was suggested that an error of 3 - 4 bar-a in predicting pressure drop might be acceptable. In this analysis, an error of 3 bar-a for pressure and 5°C for temperature was considered and getting their average would give an error value of approximately 4 bar-a °C. This error value was then used as the maximum acceptable error in evaluating the performance of the flow correlations.

In Figure 4, the distribution of the errors of each flow correlation is illustrated. Based on their histograms, Duns and Ros correlations apparently have the most satisfactory results of all correlations. However, it was observed that the Orkiszewski correlation did also perform well in simulating the given discharge data sets based on its error distribution. And it can be noticed that there is only a very little difference between the results of Orkiszewski and Duns and Ros correlations (based on their frequency of errors that is less than 4). Duns and Ros (modified by Ros) correlation comes to be third best according to its error distribution. Though, using this correlation, the possibility of getting an error (higher than the acceptable error) could be expected.

Furthermore, even though the Hagedorn and Brown correlation seems to perform well based on the number of wells matched, its error distribution suggests that there is a greater possibility that big errors would be obtained if used in simulating wells with wide range of wellhead conditions. And finally, the Armand correlation, gives unsatisfactory results based on its error distribution. It also gives poor results even without considering the error. Thus, it could be an indication that Armand correlation is not applicable to the wellhead conditions used in this study.

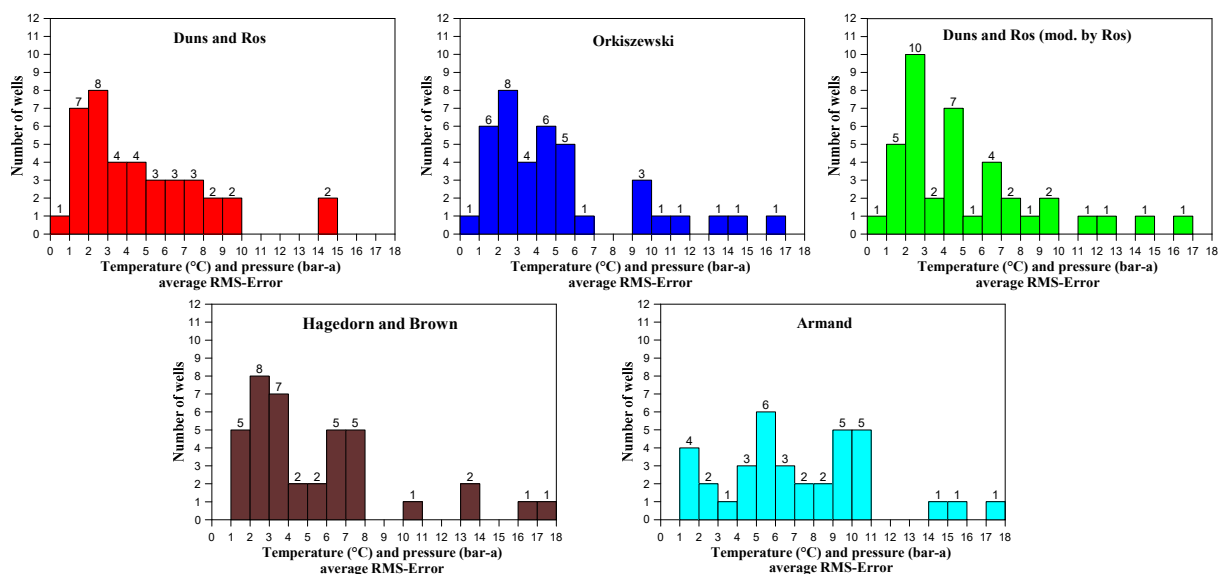


FIGURE 4: Distribution of the temperature (°C) and pressure (bar-a) average root-mean-square errors of the five flow correlations; dashed lines mark the acceptable error

The cumulative frequency distributions of the error of five flow correlations were also plotted in Figure 5. The plot shows that Duns and Ros correlation is slightly better than Orkiszewski, Hagedorn and Brown and Duns and Ros (modified by Ros) correlation, but this could be the result of statistical errors. The Armand correlation is obviously not applicable in a wide range of wellhead condition. Also, based on the plot the probability of getting an acceptable error (≈ 4 bar-a $^{\circ}$ C) using the five flow correlations are: 48% for Orkiszewski, 18% for Armand, 45% for Duns and Ros (modified by Ros) and 50% for both Duns and Ros and Hagedorn and Brown.

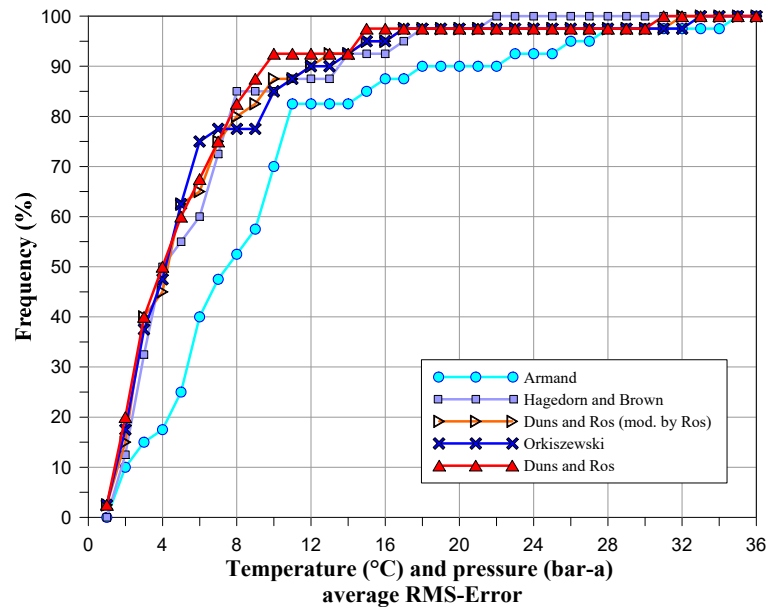


FIGURE 5: Cumulative frequency distribution of temperature and pressure average RMS-error

4.6 Performance of flow correlations based on wellhead conditions

Based on the previous analyses, it appears that Orkiszewski, Duns and Ros, Duns and Ros (modified by Ros) and Hagedorn and Brown correlations could have a general applicability in geothermal wellbore simulation. However, it would be better to identify under what conditions these flow correlations would perform the best by considering other parameters. In order to identify their applicability based on specific wellhead condition, several trials were performed such as plotting wellhead pressure versus total mass flow rate, steam fraction versus total mass flow rate and mass flow rate versus enthalpy. Then, it was observed that by plotting wellhead pressure versus wellhead steam mass flux, the wells matched by different flow correlations seem to form a cluster (see Figure 6). Steam mass flux considers different parameters at the wellhead such as dryness, enthalpy, mass flow and diameter. It can be expressed as:

$$\text{Steam mass flux} = \frac{\dot{m}_g}{\pi r^2} \tag{33}$$

where r = Radius of the well at the wellhead [m].

As illustrated in Figure 6, the wells matched by the Duns and Ros correlation mostly have wellhead pressure less than 30 bar-a and steam mass flux greater than $100 \text{ kg s}^{-1} \text{ m}^{-2}$. This means that the Duns and Ros correlation performs best under such condition. On the other hand, the Orkiszewski and the Duns and Ros (modified by Ros) correlations could be expected to produce good results if the wellhead pressure is less than 20 bar-a and the steam mass flux is higher than $100 \text{ kg s}^{-1} \text{ m}^{-2}$. Then, the wells matched by the Armand correlation apparently lie within the wellhead pressure range of 10 - 40 bar-a and less than $200 \text{ kg s}^{-1} \text{ m}^{-2}$ steam mass flux which clearly shows that Armand correlation could produce good results under such condition. Also,

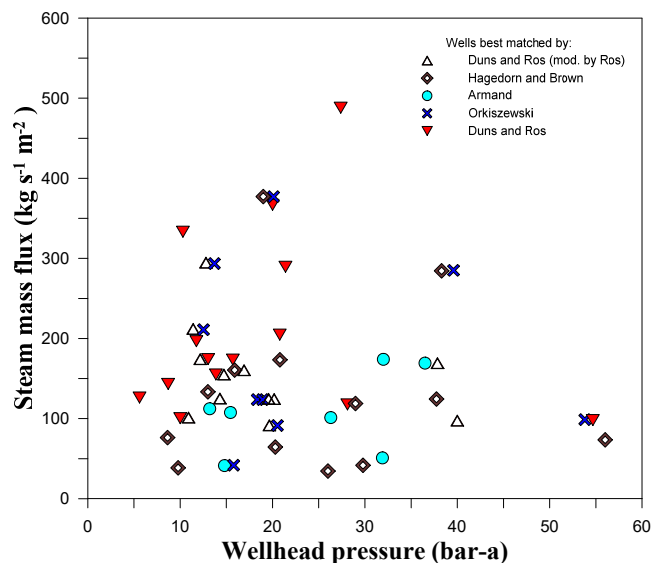


FIGURE 6: Wellhead pressure vs. steam mass flux

Hagedorn and Brown performs well under conditions almost similar to Armand correlation, with the addition that Hagedorn and Brown could match wells having wellhead pressure less than 10 bar-a. Seen in Table 4 are the conditions at the wellhead where each of the flow correlations performed well.

TABLE 4: Conditions where the different flow correlations performed well

Flow correlation	Wellhead pressure	Steam mass flux
Duns and Ros	< 30 bar-a	> 100 kg s ⁻¹ m ⁻²
Armand	10 - 40 bar-a	< 200 kg s ⁻¹ m ⁻²
Orkiszewski	< 20 bar-a	> 100 kg s ⁻¹ m ⁻²
Duns and Ros (mod. by Ros)	< 20 bar-a	> 100 kg s ⁻¹ m ⁻²
Hagedorn and Brown	< 40 bar-a	< 200 kg s ⁻¹ m ⁻²

4.7 Performance of flow correlations based on wellhead enthalpy

The flow correlations were also evaluated based on the enthalpy of the well. In this analysis, the classification of wells based on wellhead dryness mentioned in Section 4.1 was used. Out of 40 wells, 29 have enthalpy less than 1500 kJ/kg while the rest have enthalpy ranging from 1500 to 2500 kJ/kg. This is to identify which correlation will give a good result in reproducing the flowing pressure and temperature of a well having an enthalpy less than 1500 kJ/kg or in the range 1500 - 2500 kJ/kg. In Figure 7, the mean errors obtained by the flow correlations on two classifications of wellhead enthalpy or dryness are illustrated. Duns and Ros correlation noticeably gives the most accurate result in wells having an enthalpy ranging from 1500 to 2500 kJ/kg. For wells with less than 1500 kJ/kg enthalpy, the result suggests that all correlations except Armand could give good results.

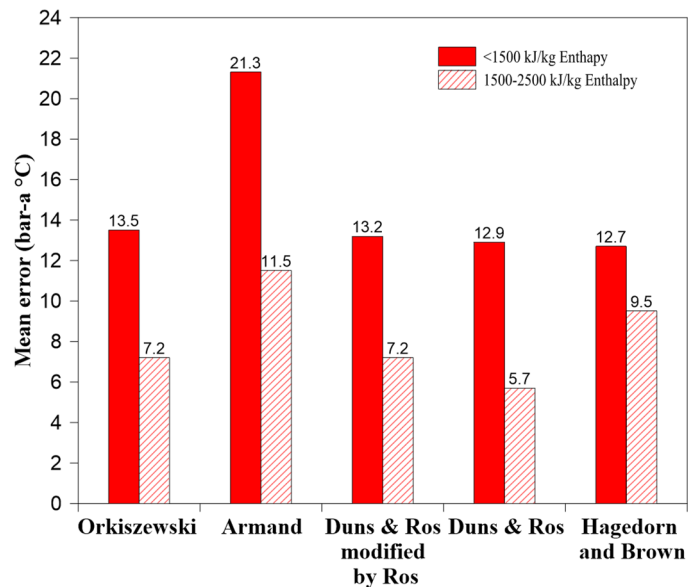


FIGURE 7: Performance of flow correlations on wells having an enthalpy of < 1500 kJ/kg and 1500 - 2500 kJ/kg

4.8 Performance of flow correlations based on fluid flow regime

An analysis was performed to identify the reason why other correlations did not perform well with the given sets of discharge data. Since all of the correlations which performed well, except Hagedorn and Brown (1965), are dependent on the pressure drop calculated assuming a certain flow regime, this could be one of the reasons why other correlations have unsatisfactory results. Hence, it was decided to use flow regime map to predict the flow pattern of the fluid flowing through the wells.

The flow regime map is one of the commonly used maps in predicting flow patterns for inclined flow. It was developed by Aziz et al., (1972), but here it is based on the paper of Ehizoyanyan et al. (2015). Initially, the superficial velocities of the two phases obtained from the simulation using each correlation were plotted to verify if there was a difference with the predicted flow regimes for each correlation. Then it was observed that the flow correlations were producing almost the same fluid flow regimes

throughout the cased-off section of the wells. An example of this is shown in Figure 8 where well 21 is experiencing slug flow at the top of liner and annular/mist flow at the wellhead while well 34 has an annular/mist flow from top of liner up to the wellhead. It was also observed that the flow correlations produce almost the same superficial velocities of liquid and gas at the top of liner of the wells. And Orkiszewski, Duns and Ros and Duns and Ros (modified by Ros) correlations calculate the same value of superficial velocities of the two phases throughout the cased-off section of the wells.

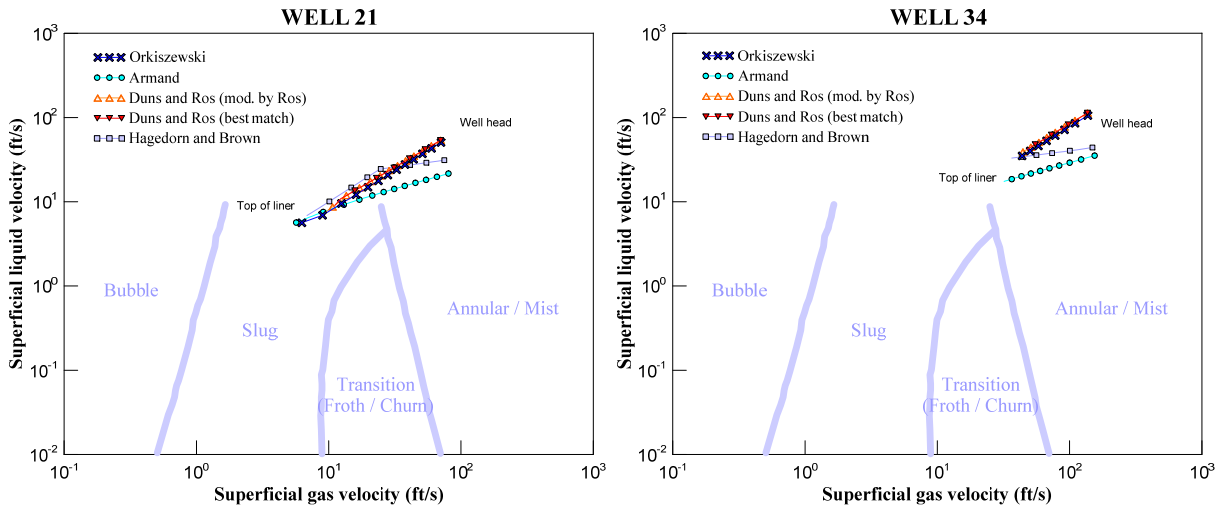


FIGURE 8: Predicted flow regimes of the fluid throughout the cased-off section of well 21 and well 34 based on Aziz et al., (1972) flow pattern map

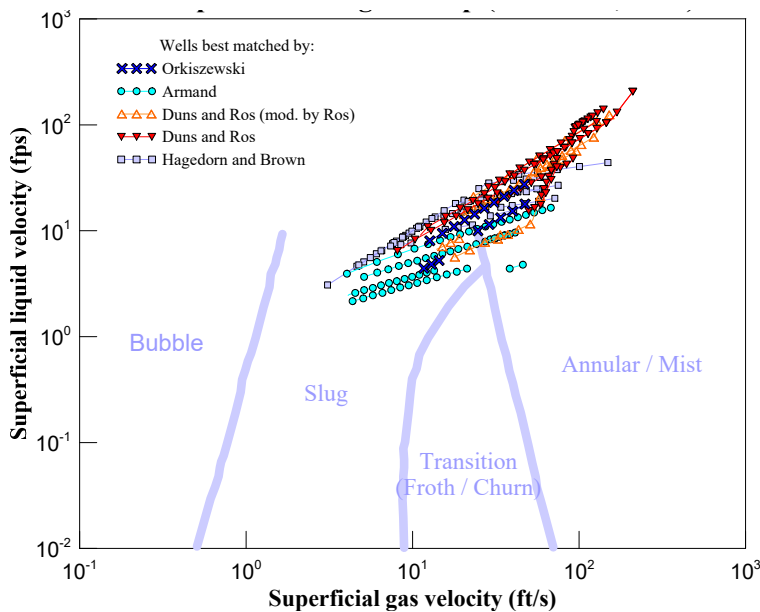


FIGURE 9: Predicted flow regimes of the fluid throughout the cased-off section of the wells based on Aziz et al., (1972) flow pattern map

To check the fluid flow regime of all of the wells, the same process was repeated, though in this case the superficial velocities of the two phases based on the well's best matched correlation were used (see Figure 9). And it was observed that most portions of the wells were experiencing annular/mist flow. According to Bellarby (2009), the Duns and Ros correlation gives an accurate result in predicting the pressure drop of two-phase fluid flow specifically in mist flow. This could be the reason why the Duns and Ros correlation performs best of the correlations. Likewise, Orkiszewski and Duns and Ros (modified by Ros) correlations also performed well because both used the method of Duns and Ros correlation in mist flow. It is also noted that the Armand correlation

seems to have a good performance on wells which have lower superficial liquid velocity (slug flow). And the Hagedorn and Brown correlation, although it does not consider the flow regime in pressure drop calculations, still gives good matches for wells experiencing slug and annular/mist flow. Lastly, the Armand correlation seems to perform well in slug flow which also agrees with the study of Spedding and Chen (1982) that the Armand correlation is only applicable to bubble and slug flow regimes.

5. CONCLUSIONS AND RECOMMENDATIONS

In this study, different analyses were performed to evaluate and compare the performance of different flow correlations as implemented in EDC's in-house simulator Simgwel. Based on these analyses, it can be concluded that each flow correlation has a different applicability depending on the condition of the fluid in the wellbore up to the wellhead. The accuracy of flow correlations in simulating flowing pressure and temperature profiles of a geothermal well may greatly depend on the condition of the fluid and its flow regime. The Duns and Ros correlation gives an accurate result if the fluid flow regime is mist. And based on the 40 sets of discharge data that were simulated, it would give good matches between the calculated and measured profiles if the steam mass flux is higher than $100 \text{ kg s}^{-1} \text{ m}^{-2}$ and wellhead pressure is less than 30 bar-a.

The Orkiszewski correlation gives good results if used in mist flow and would also perform well in simulating geothermal wells having wellhead pressure of less than 20 bar-a and steam mass flux greater than $100 \text{ kg s}^{-1} \text{ m}^{-2}$. Duns and Ros (based on Ros) correlation also performs well in mist flow but there is still a possibility that it will give unsatisfactory results. It can also produce accurate results if the wellhead pressure is less than 20 bar-a and the steam mass flux higher than $100 \text{ kg s}^{-1} \text{ m}^{-2}$. The Hagedorn and Brown correlation on the other hand, can give a good match on wells with wellhead pressure less than 40 bar-a and steam mass flux less than $200 \text{ kg s}^{-1} \text{ m}^{-2}$. However, it should be used with caution because of the possibility that it may give a significantly large error. Furthermore, the performance of Armand correlation is unsatisfactory based on the error obtained between the measured and predicted flowing profiles. Although, it may give good results if the steam mass flux at the wellhead is less than $200 \text{ kg s}^{-1} \text{ m}^{-2}$, further evaluation is necessary to confirm this result.

In conclusion, it should be noted that these evaluations still need to be validated through an intensive study having a substantial amount of data and considering other important parameters such as chemical composition of the fluid (non-condensable gas content and total dissolved solids) and casing blockage or scale. In the case of modelling a geothermal well, it is recommended to first predict the fluid flow regime. This would help the reservoir engineer to decide what flow correlation to use.

ACKNOWLEDGEMENTS

Sincere gratitude is hereby extended to the following who have never ceased to support and helped me in all aspects throughout my venture and until this paper is structured:

To Mr. Lúdvík S. Georgsson, director of UNU-GTP and Mr. Ingimar Gudni Haraldsson, deputy director of UNU-GTP, for the opportunity to participate in the six-month training programme. To the UNU-GTP staff, Markús, Frída and Thórhildur, thank you for all of your precious time and efforts that guided us through life in Iceland. To Rósa Jónsdóttir, thank you for sending me the copy of all the books and references that I needed.

To my supervisors Mr. Lárus Thorvaldsson and Dr. Jean-Claude Berthet whose expertise and guidance highly contributed to the success and completion of this study. To Valdís Gudmundsdóttir and my colleagues in EDC, Yam Alcaraz, Julius Rivera and Daryl On, thank you for sending me all the data that I needed. To Ms. Kristine Eia Antonio, thank you for all the encouragements, comments, patience and effort in checking this study. To Mr. Jaime Austria, thank you for checking and sharing your ideas for the project. To Ms. Selna Marquez, for also sharing your ideas in this study, thank you very much.

To the management of the Energy Development Corporation, President Richard Tantoco and GREG SVP Manny Ogena, thank you for supporting me in this training. To Mr. Francis Sta. Ana, Mr. Dave Yglopaz, Mr. Jericho Omagbon and Mr. Anthony Ciriaco, thank you for nominating me for this training.

To my brothers here in Iceland, Jigo Mismanos, Jason Gotuato and Lee Monasterial, thank you for all the good times and experiences we have shared together that made my stay more enjoyable and unforgettable here in Iceland.

To my parents Reynaldo and Nora and my siblings Reygie, Roxanne, Niño and Beverlyn who are my motivations to give my best to finish this work. To all my friends and Church mates, for the unwavering moral support and words of encouragements that helped me pull through, thank you very much. To my beloved Ms. Jemimah Keren Rivera, thank you for all the encouragements and taking time to help me finish this project.

Above all, utmost appreciation offers to my GOD Almighty for the divine favour and for giving me strength throughout this journey. With You, all things are possible.

REFERENCES

- Ambastha, A.K., and Gudmundsson, J.S., 1986: Pressure profiles in two-phase geothermal wells: Comparison of field data and model calculations. *Proceedings of the 11th Workshop on Geothermal Reservoir Engineering, Stanford University, Stanford, CA, United States*, 183-188.
- Armand, A.A., 1946: *The resistance during the movement of a two-phase system in horizontal pipes*. *Izv. Vses. Teplotek. Inst.*, Vol. 1, 16-23.
- Aunzo, Z., Björnsson, G., and Bödvarsson, G., 1991: *Wellbore models GWELL, GWNACL, and HOLA user's guide*. Lawrence Berkeley Laboratory, Berkeley, CA, United States, report LBL-31428 / UC-251, 102 pp.
- Aziz, K., Govier, G.W., and Fogarasi, M., 1972: Pressure drop in wells producing oil and gas. *J. Canadian Petroleum Technology*, 11, 31-38.
- Barelli, A., Corsi, R., Del Pizzo, G., and Scali, C., 1982: A two-phase flow model for geothermal wells in the presence of non-condensable gas, *Geothermics*, 11, 175-191.
- Bellarby, J., 2009: *Well completion design*. Elsevier, 711 pp.
- Bhat, A., Swenson, D., and Gosavi, S., 2005: Coupling the HOLA wellbore simulator with TOUGH2. *Proceedings of the 30th Workshop on Geothermal Reservoir Engineering, Stanford University, Stanford, CA, US*, 3-6.
- Björnsson, G., 1987: *A multi-feedzone geothermal wellbore simulator*. University of California / Lawrence Berkeley Laboratory, MSc thesis, report LBL-23546, 102 pp.
- Carrascal, J.F., 1996: *Multiphase flow application to esp pump design program*. Texas Tech University, Thesis in Petroleum Engineering, 134 pp.
- Duns Jr., H., and Ros, N.C.J., 1963: Vertical flow of gas and liquid mixtures in wells. *Proceedings of the 6th World Petroleum Congress, Frankfurt am Main, Germany*, 22-106.
- Ehizoyanyan, O., Appah, D., and Sylvester, O., 2015. Estimation of pressure drop, liquid holdup and flow pattern in a two phase vertical flow. *International J. Engineering and Technology*, 4, 241-253.
- Fajardo, V.R., and Malate, R.C.M., 2005: Estimating the improvement of Tanawon production wells for acid treatment, Tanawon sector, BacMan geothermal production field, Philippines. *Proceedings of the World Geothermal Congress 2005, Antalya, Turkey*, 5-7.
- Freeston, D., and Hadgu, T., 1988: Comparison of results from some wellbore simulators using a databank. *Proceedings of the 10th New Zealand Geothermal Workshop, Auckland University, Auckland, NZ*, 4-7.

- Freeston, D., and Gunn, C., 1993: Wellbore simulation – case studies. *Proceedings of the 18th Workshop on Geothermal Reservoir Engineering, Stanford University, Stanford, CA, US*, 3-6.
- Gould, T., 1974: Vertical two-phase steam-water flow in geothermal wells. *J. Petroleum Technology*, 26, 833-842.
- Griffith, P., and Wallis, G.B., 1961: Two-phase slug flow. *J. Heat Transfer*, 83, 307-318.
- Gudmundsdóttir, H., 2012: *A coupled wellbore-reservoir simulator utilizing measured wellhead conditions*. University of Iceland, MS thesis, 119 pp.
- Hagedorn, A.R., and Brown, K.E., 1965: Experimental study of pressure gradients occurring during continuous two-phase flow in small diameter vertical conduits. *J. Petroleum Technology*, 4, 475-484.
- Hsu, Y.Y., and Graham, R.W., 1976: *Transport processes in boiling and two-phase systems*. Hemisphere Publishing Corp., NY, US, 559 pp.
- Koehler, A., and Koehler, H.R., 2006: Another look at measures of forecast accuracy. *International J. Forecasting*, 22, 679–688.
- Lyons, W., 2010: *Working guide to petroleum and natural gas production engineering*. Elsevier, Oxford, United Kingdom, 316 pp.
- Marquez, S., Sazon, T.A., Omagbon, J., and Sazon, T.A., 2015: SIMGWEL: EDC's new geothermal wellbore modeling software. *Proceedings of the World Geothermal Congress 2015, Melbourne, Australia*, 4 pp.
- McGuinness, M.J., 2013: *Geothermal wellbore simulation*. Short Course on Geothermal Well Bore Simulation, held for Energy Development Company, Manila, Philippines.
- McGuinness, M.J., 2014: *Simgwel User Manual Version 9.10*. Wellington: Marsan Consulting Ltd.
- Orkiszewski, J., 1967: Predicting two-phase pressure drops in vertical pipes. *J. Petroleum Technology*, 19, 829-838.
- Pálsson, H., 2011: *Simulation of two-phase flow in a geothermal well*. University of Iceland, lecture notes, 8 pp.
- Probst, A., Gunn, C., and Andersen, G., 1992: A preliminary comparison of pressure drop models used in simulating geothermal production wells. *Proceedings of the 14th New Zealand Geothermal Workshop, Auckland, NZ*, 139-144.
- Ravindran, N., and Horne, R., 1993: *Multivariate optimization of production systems - the time dimension*. Stanford University, Petroleum Research Institute, Stanford, CA, US, report DOE/BC/14600-42, 114 pp.
- Ros, N.C.J.: 1961: Simultaneous flow of gas-liquid as encountered in well-tubing. *J. Pet. Tech.*, 10, 37-49.
- Spedding, P.L., and Chen, J.J.J., 1982: *Holdup in inclined two-phase flow*. University of Auckland and University of Hong Kong, 7 pp.
- Tanaka, S., and Nishi, K., 1988: Computer code of two-phase flow in geothermal wells producing water and/or water-carbon dioxide mixtures. *Proceedings of the 13th Workshop on Geothermal Reservoir Engineering, Stanford University, Stanford, CA, US*, 159-164.
- Thórisdóttir, Th.H., 2013: *Estimation of slip ratios for pressure drop calculations in geothermal wells*. University of Iceland, MSc thesis, 50 pp.
- White, F.M., 1979: *Fluid mechanics*. McGraw-Hill, NY, US, 847 pp.